Petroleum and Coal

Article **Open Access**

RESOLUTION OF SEISMIC INTERPRETATION ANOMALIES THROUGH THE SPECTRAL RATIO TIME DEPENDENT METHOD

Moses E. Emetere, Caleb T. Oritseneyemi, Omotayo O. Ojo

Department of Physics, Covenant University, Canaan land, P.M.B 1023, Ota-Nigeria

Received April 1, 2017; Accepted May 31, 2017

Abstract

Interpretation of seismic results from a complex geological formation can be very difficult both on-field and off-field. The spectra ratio (SR) time-dependent method was derived using established geological principles. The spectral amplitude was analyzed numerically to affirm the reliability of the method on field operations. It was observed that the SR time-dependent method could initiate a natural correction to the attenuated seismic amplitude at each given interval during a seismic operation. The multi-layer implementation of the adopted method showed great success with the most accurate result at n = 0.1 for the fourth term on a newly-propounded volumetric table. Most volumetric results from the Niger-Delta showed correspondence with the volumetric analysis of the fourth term. One of the on-field volumetric results was obtained in the third term. The derivation of the volumetric table is to further enhance more accurate exploration using the reflective seismic technique.

Keywords: *spectra ratio, volumetric table, Niger-Delta, spectral amplitude, numerical analysis*.

1. Introduction

The results from seismic exploration have widely varying degrees of uncertainty and many important aspects still remain mysterious [1]. The in-homogeneities within the sub-surface are highly anisotropic in interpreting faults, structural deformation and depositional environments. Hence, the modelling and analysis of wave propagation in the earth's crust could be somewhat challenging mathematically because it leads to wave localization amongst other challenges. This occurrence greatly influences the resolution of seismic imaging and also the effective depth of seismic probes. There are no 'good enough' transport theoretic boundary conditions to describe the earth's surface and interfaces. In exploration seismology, where seismic probing can generate huge data sets, not so much good algorithms for imaging exist. Efficient compression of geophysical data sets is perhaps the most urgent problem that exploration seismology faces at present. The theory of elasticity is used to explain the propagation of seismic waves. However, materials may respond differently to brief and sudden stress than they would to long lasting steady stress. The stress response of minerals and rocks (geo materials) in the earth's interior is affected by many other factors, including temperature, hydrostatic confining pressure, and time [2]. Hence they show elastic, inelastic and plastic behaviour with various degrees of importance at different depth. The major phenomenon in the theory of seismic waves relate to the difficulties as a result of uneven distribution of materials in the earth surfaces in which geologist refer to as inhomogeneities, and this is not the only cause in seismology. Inelastic behaviour in the subsurface is related to the petrophysical properties of geo-materials. The amplitude attenuation is as a result of the inelastic damping of the vibration of the particle of the materials. The theory of propagation of seismic waves is built by considering the behaviour of an elastic medium when stresses travel through it. Both transverse and longitudinal waves can be propagated through solids. Seismic body waves can either be longitudinal waves (primary waves) or transverse waves (secondary waves). The two common types of waves common in seismology are P waves and S waves, involve respectively condensation rare fractional and distortional motion. P waves possess the ability to penetrate geological layers with only a few reflected by lithologic interfaces. P waves are not independent on their own because it has the challenge of imaging subsalts, formations beneath volcanic rocks, formations with low acoustic impedance contrast [3]. The S waves information are required to adequately solve seismic imaging or reservoir properties as shown in Figure 1.

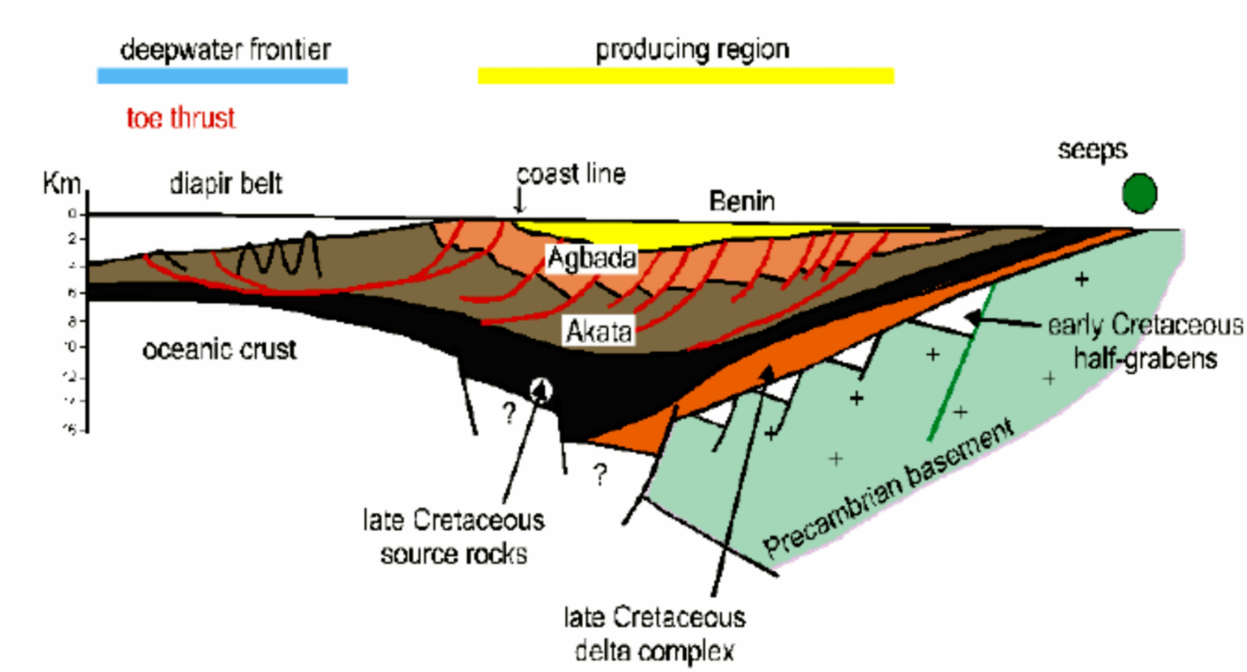

Figure 1. Cross section of Niger-Delta formation [22]

The peculiarities in the Niger-Delta which includes a dynamic petroleum system is a clear indication that static exploration approach maybe outdated and irrelevant in drawing research conclusion as seen in recent research. This suggests that the yet undiscovered hydrocarbon deposit in a complex geological environment requires not just a higher resolution seismic reflection method but an improved Q-factor which is largely dependent on the spectral amplitude. The degree of seismic attenuation is measure by the Q-factor. Li *et al.* [4] placed more emphasis on the Q-estimation which is dependent on the frequency shift method. Their method was basically to control the phase spectrum to prevent the stress on the seismic wavelet and the exponential decay of seismic amplitude with respect to time or depth. The inhomogeneities of the complex geology of the Niger-Delta are supposed to dissipate high-frequency seismic energy and a corresponding decrease in the seismic amplitude. However, the sudden seismic amplitude decrease is clear evidence that it may depend on scattering, radius of convergence from seismic source, variation with illumination angle, geometric spreading. Unfortunately, this factors can be related to the frequency which is a major indictment to the frequency -based methods. In agreement with recent research [4], spectral ratio (SR) method is more viable. Unlike the earlier research, we seek to modify the SR method as a function of time which may be salient for resolving anomalies in reservoir depth among others. The focus of this research shall be the Niger Delta, Nigeria, West Africa.

2. Background theories and formulation

The physics of the spectral amplitude $A_o(f)$ modified to $A_n(f)$ at time (t) and frequency (f) is given as

$$A_n(f) = A_o(f)\exp(-\frac{\pi f t}{Q}) \qquad (1)$$

In this research we are more interested in the multilayer implementation; hence, it was assumed that the spectral amplitude has a differential impact as it transmits. This can be expressed using the hermit polynomial

$$\sum_{n=0}^{\infty} \frac{A_n(f)}{A_o(f)} r^n = \exp(-\frac{\pi f t}{Q}) \qquad for\ |r| < \infty \tag{2}$$

We represent $x = -\frac{\pi f t}{Q}$ and expand the exponential using the Maclaurin's series i.e.

$$\exp(x) = x^n + \frac{x^n}{(n+1)!} + \frac{x^{2n}}{(n+2)!} + \frac{x^{3n}}{(n+3)!} \ldots \ldots \ldots \ldots \tag{3}$$

Hence, equation (2) becomes

$$\sum_{n=0}^{\infty} \frac{A_n(f)}{A_o(f)} r^n = x^n + \frac{x^n}{(n+1)!} + \frac{x^{2n}}{(n+2)!} + \frac{x^{3n}}{(n+3)!} \tag{4}$$

where r^n is the radius of convergence. The relationship between frequency fluctuation and the symmetry of the seismic source is significant in live seismic probe [5]. Therefore, high frequency must be avoided by tuning the radius of convergence to unity. This gives a broader outlook on the multi layer implementation of the amplitude spectrum shown below

$$A_n(f,t) = \begin{cases} A_o(f,t)x^n & x^n = -x^n\ for\ n \le 0.6 \\ A_o(f,t)\frac{x^n}{(n+1)!} & x^n = -x^n\ for\ n \le 0.6 \\ A_o(f,t)\frac{x^{2n}}{(n+2)!} & x^n = -x^n\ for\ n \le 0.3 \\ A_o(f,t)\frac{x^{3n}}{(n+3)!} & x^n = -x^n\ for\ n \le 0.2 \end{cases} \tag{5}$$

This parametric spectral amplitude would be very useful to analyze the differential compaction of either the incised channel engraved in shales or the incised channel engraved in sand [6]. This may be a good way of detecting depositional environment and structural deformation. Taking the peculiar case of the Niger-Delta formation that is characterized by a transitional shale diapir controlled system, roll over anticlines and extensional growth fault [7], there is the need to know the amplitude misfit function per time. Ritsema *et al.* [8] gave amplitude misfit function which was modified to

$$\chi(f,t) = \frac{1}{2}\sum_{n=1}^{\infty}\left[\frac{A_n(f,t)}{A_o(f,t)} - 1\right]^2 \tag{6}$$

and the new gradient (with respect to time) given as

$$\delta\chi(f,t) = \frac{n}{t}\sum_{n=1}^{\infty}\left[\frac{A_n(f,t)}{A_o(f,t)} - 1\right]\delta t \tag{7}$$

The modified spectral amplitude can be adopted into the volume analysis for adequate estimation of reservoir thickness and pore space [9]. Hence, the various pore volume can be determine using uni-layer

$$V_n = A\varphi.\frac{sQ}{\pi f t}\sum_{n=1}^{\infty}\sqrt[n]{\frac{A_n(f,t)}{A_o(f,t)}} \tag{8}$$

where A is the area of the pore area, s is the speed of the seismic event, φ is the porosity.

3. Geological background of study area

Most research on Niger-Delta is closely within the border of longitude 3.11° – 9.03° and latitude 4.21° – 5.03°. In general, it is made of three formations – Akata, Agbada and Benin formations as illustrated earlier in Figure 1. Basically, the Benin formation is made-up of sand and gravel (as the shallowest formation); the layer below – Agbada formation is made up of sand and shale; the deepest layer is the Akata formation is comprised of shale, sand and silt. The origin of each formation from literature may be very complex to articulate [7,9-11]. The thickness of the regressive clastic sequence is still unknown but could be estimated-from literature to have a minimum of 6,000 m [9,12-14]. The thickness of each formation should have a minimum of 1200 m. The marine shale facies between the upper Akata formation and the lower Agbada formation are evidences of primary source rocks whose properties have been described by the aforementioned literatures. The development of traps, growth faults and crest structures is dynamic. Hence, the petroleum system over Niger-Delta may not be static in description and literature must be updated to capture its trend per time. Kulke [15] calculate the area of the largest regression in the Niger Delta as 300,000 km^2. Since Niger-Delta is a sedimentary basin, it necessary to understand the extent of the basic formations. Michele *et al.* [16] calculated the sediment volume and thickness as 500,000 km^3 and 10 km respectively.

4. Numerical analysis of the Spectra Amplitude on the Niger-Delta Field

The parameters adopted in this section were obtained from Barton [17] i.e. the Q factor between 26-200. The frequency is between 450-725 Hz. Though the travel time of S waves through the sedimentary rock was estimated by Campbell [18] to be 1.10 sec, we considered maximum time of 4 sec to account for site attenuation parameter which may be dependent on either the maximum frequency [19-20] or corner frequency. The spectral amplitude was considered to gradually decrease with respect to the depth of the inhomogeneous subsurface. We monitored the decrease trends of the SR- method with respect time. We suggest that the trend is a vital parameter for understanding the deposit in a complex geology as Niger Delta.

We maintain the A_n output using the gradient of the amplitude misfit function ($\delta\chi$) which should not be above 8 as shown in Table 1 and 2 which was obtained from the first and second term of the spectra amplitude analysis in equation (5). When A_o is unity, then $A_o \approx -\frac{\pi f t}{Q}$. This an important resolution which explains that maximum frequency do not have significant effect on the site attenuation parameter, hence, the intrinsic attenuation or anelasticity are dominant. We considered the n-term within $0.1 \le n \le 0.3$ and $0.4 \le n \le 0.6$. When $0.1 \le n \le 0.3$ (Table 1), the spectral amplitude ratio increase with respect to time or depth. This occurrence may be an advantage in reflection seismic method to determine deposit in difficult terrains. The $\delta\chi$ was below 0.4 at this state. Hence, for multilayer implementation, the different seismic sounding is best when $\delta\chi$ is below 0.5.

Table 1. First and second term of the spectra amplitude analysis at $0.1 \le n \le 0.3$

Basic Parameters of the first order					$n = 0.1$, $\delta\chi = 0.019$		$n = 0.2$, $\delta\chi = 0.12$		$n = 0.3$, $\delta\chi = 0.40$	
A_o	$t\ (s)$	Q	$f\ (Hz)$	$\frac{\pi f t}{Q}$	A_n	$\frac{A_n(f,t)}{A_o(f,t)}$	A_n	$\frac{A_n(f,t)}{A_o(f,t)}$	A_n	$\frac{A_n(f,t)}{A_o(f,t)}$
1	10	26	450	1.88	1.88	1.88	3.52	3.52	6.62	6.62
0.9	30	46	480	1.99	1.79	1.99	3.57	3.97	7.11	7.9
0.8	60	66	510	2.07	1.66	2.07	3.43	4.29	7.11	8.89
0.7	90	86	540	2.11	1.48	2.11	3.13	4.46	6.6	9.43
0.6	120	106	570	2.14	1.28	2.14	2.75	4.58	5.89	9.82
0.5	150	126	600	2.16	1.08	2.16	2.34	4.68	5.06	10.1
0.4	180	146	630	2.18	0.87	2.18	1.9	4.76	4.15	10.4
0.3	210	166	660	2.2	0.66	2.2	1.45	4.83	3.18	10.6
0.2	240	186	690	2.21	0.44	2.21	0.98	4.89	2.16	10.8
0.1	270	200	720	2.23	0.22	2.23	0.5	4.98	1.11	11.1

Also, as the 'n' term increases, the spectra amplitude ratio increases. Therefore, under a controlled seismic process, when high-frequency seismic energy are administered, a decrease in the seismic amplitude occurs, however, there is a corresponding increase in the spectra amplitude ratio in a multi-layer implementation. This idea further affirms the advantage of the SR method in exploration activities. When $0.4 \le n \le 0.6$(Table 2), it is observed that the SR-time dependent method stabilizes fluctuation or attenuation noticed in A_n at any depth or time.

Table 2. First and second term of the spectra amplitude analysis at $0.4 \le n \le 0.6$

Basic Parameters of the first order					$n = 0.4,\ \delta\chi = 1.14$		$n = 0.5,\ \delta\chi = 2.96$		$n = 0.6,\ \delta\chi = 7.28$	
A_o	$t\ (s)$	Q	$f\ (Hz)$	$\frac{\pi f t}{Q}$	A_n	$\frac{A_n(f,t)}{A_o(f,t)}$	A_n	$\frac{A_n(f,t)}{A_o(f,t)}$	A_n	$\frac{A_n(f,t)}{A_o(f,t)}$
1	10	26	450	1.88	12.4	12.4	23.3	23.3	43.8	43.8
0.9	30	46	480	1.99	14.2	15.7	28.2	31.4	56.2	62.4
0.8	60	66	510	2.07	14.7	18.4	30.5	38.2	63.2	79
0.7	90	86	540	2.11	14	19.9	29.5	42.1	62.3	89
0.6	120	106	570	2.14	12.6	21	27	45	57.8	96.4
0.5	150	126	600	2.16	10.9	21.9	23.7	47.4	51.2	102
0.4	180	146	630	2.18	9.06	22.6	19.8	49.4	43.1	108
0.3	210	166	660	2.2	6.99	23.3	15.4	51.2	33.7	112
0.2	240	186	690	2.21	4.78	23.9	10.6	52.9	23.4	117
0.1	270	200	720	2.23	2.48	24.8	5.52	55.2	12.3	123

It was also observed that when $0.4 \le n \le 0.6$, $\delta\chi > 1$, hence at higher multilayer implementation, the tendency of a higher misfit which may be error prone. We observed the misfit trends for the multilayered terms in Figure 2. While $0.1 \le n \le 0.3$ the misfit trend is near perfect, the accuracy when n = 0.4 may be reliable in exploration. The accuracy of $n \ge 0.5$ is somewhat questionable.

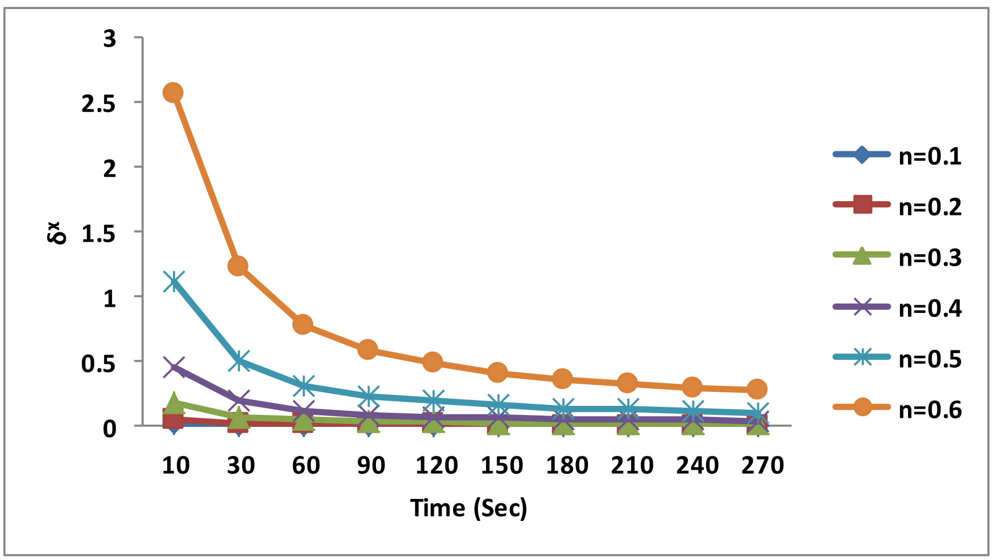

Figure 2: Misfit trends in a multi-layered SR-time dependent method

The third term spectra amplitude analysis at $0.1 \le n \le 0.3$ was considered as shown in Table 3. The accuracy for the third term spectra analysis was within $0.1 \le n \le 0.2$. The accuracy at first and second term is the same with third term at n = 0.019. As shown in the previous tables, the third term could also stabilized fluctuation or attenuations on the amplitude per time or depth. The fourth term spectra amplitude analysis at $0.1 \le n \le 0.3$ was considered as shown in Table 4. Like the third term, the accuracy was within $0.1 \le n \le 0.2$. The most accurate result was discovered at n = 0.1 of the fourth term. Hence, it is preferably to test the fourth term of the SR-time dependent method. In the next session we shall be applying the SR-time dependent method in a known oil field in Niger-Delta.

Table 3. Third term spectra amplitude analysis at $0.1 \le n \le 0.3$

Basic Parameters of the first order					$n = 0.1$, $\delta\chi = 0.019$		$n = 0.2$, $\delta\chi = 0.27$		$n = 0.3$, $\delta\chi = 1.79$	
A_o	$t\ (s)$	Q	$f\ (Hz)$	$\frac{\pi f t}{Q}$	A_n	$\frac{A_n(f,t)}{A_o(f,t)}$	A_n	$\frac{A_n(f,t)}{A_o(f,t)}$	A_n	$\frac{A_n(f,t)}{A_o(f,t)}$
1	10	26	450	1.88	1.76	1.76	6.21	6.21	21.9	21.9
0.9	30	46	480	1.99	1.79	1.98	7.08	7.87	28.1	31.2
0.8	60	66	510	2.07	1.72	2.15	7.37	9.21	31.6	39.5
0.7	90	86	540	2.11	1.56	2.23	6.98	9.97	31.2	44.5
0.6	120	106	570	2.14	1.38	2.29	6.31	10.5	28.9	48.2
0.5	150	126	600	2.16	1.17	2.34	5.47	10.9	25.6	51.2
0.4	180	146	630	2.18	0.95	2.38	4.53	11.3	21.5	53.9
0.3	210	166	660	2.2	0.72	2.41	3.5	11.7	16.9	56.2
0.2	240	186	690	2.21	0.49	2.44	2.39	12	11.7	58.5
0.1	270	200	720	2.23	0.25	2.49	1.24	12.4	6.16	61.6

Table 4. Fourth term spectra amplitude analysis at $0.1 \le n \le 0.3$

Basic Parameters of the first order					$n = 0.1$, $\delta\chi = 0.006$		$n = 0.2$, $\delta\chi = 0.37$		$n = 0.3$, $\delta\chi = 5.11$	
A_o	$t\ (s)$	Q	$f\ (Hz)$	$\frac{\pi f t}{Q}$	A_n	$\frac{A_n(f,t)}{A_o(f,t)}$	A_n	$\frac{A_n(f,t)}{A_o(f,t)}$	A_n	$\frac{A_n(f,t)}{A_o(f,t)}$
1	10	26	450	1.88	1.1	1.1	7.29	7.29	48.3	48.3
0.9	30	46	480	1.99	1.19	1.32	9.37	10.4	74	82.2
0.8	60	66	510	2.07	1.19	1.48	10.5	13.2	93.7	117
0.7	90	86	540	2.11	1.1	1.57	10.4	14.8	98	140
0.6	120	106	570	2.14	0.98	1.64	9.64	16.1	94.6	158
0.5	150	126	600	2.16	0.84	1.69	8.54	17.1	86.4	173
0.4	180	146	630	2.18	0.69	1.73	7.18	18	74.5	186
0.3	210	166	660	2.2	0.53	1.77	5.62	18.7	59.7	199
0.2	240	186	690	2.21	0.36	1.8	3.9	19.5	42.1	211
0.1	270	200	720	2.23	0.19	1.85	2.05	20.5	22.8	228

5. Application to the field data

The fields considered in this session is located in Niger-Delta and christened X-field. This section is aimed at estimating the volumetric analysis of hydrocarbon reserves. The porosity was given as 32.5%, the area of the reservoir was given as 5.29 km^2 [14]. The volumetric table for multi-layer implementation was generated from equation (8) as shown in Table 5.

The volume obtained from Ameloko and Owoseni [21] for the total Gross Rock Volume is shown on the green box in Table 5. This means that seismic reflection parameters within same field could generate any result within the column. For example, the volume of hydrocarbon obtained by Aigbedion and Aigbedion [22] can be found in the yellow box in Table 5. The two outcomes gotten by the authors correspond sequentially with volumetric table. Similarly the result of Ihianle *et al.* [9] falls within the same column (blue box) as Aigbedion and Aigbedion [22]. Intuitively, the volume of a hydrocarbon reserves could originate two columns either within same term or dissimilar terms. The importance of the volumetric table is to further affirm the results reflective seismic technique. It enables researcher to determine the q-factor of results for further probe; it enables the determination of depth of reservoir via the SR-time dependent method; and it enables the estimation of the areal extent of the hydrocarbon accumulation.

Table 5. Volumetric table for multi-layer implementation

$t\ (s)$	Second Term Volume analysis $V_{0.1,0.2,0.3}$	Third term Volume analysis $V_{0.1}$	$V_{0.2}$	$V_{0.3}$	Fourth term Volume analysis $V_{0.1}$	$V_{0.2}$	$V_{0.3}$
10	3458	1835.244	58727.81	186449.2	16.8908	131342.8	2602107
30	3458	3319.398	106220.7	337229.8	55.25621	429672.3	8512480
60	3458	4916.23	157319.4	499457.8	121.2067	942503.6	18672470
90	3458	5992.286	191753.1	608778.3	180.0725	1400244	27741020
120	3458	6842.344	218955	695138.8	234.786	1825696	36169896
150	3458	7574.023	242368.8	769472.8	287.684	2237031	44319078
180	3458	8235.972	263551.1	836722.6	340.167	2645139	52404331
210	3458	8853.395	283308.6	899448.8	393.081	3056598	60555984
240	3458	9440.654	302100.9	959110.6	446.9578	3475544	68855964
270	3458	10306.73	329815.4	1047099	532.7265	4142481	82069033

6. Conclusion

The SR time-dependent method is reliable in that it initiates a natural correction to the attenuated seismic amplitude. Also, the multi-layer implementation showed great success with the most accurate result at n = 0.1 for the fourth term. Most volumetric results from the Niger-Delta showed correspondence with the volumetric analysis for the fourth term. One of the volumetric result was obtained in the third term. This further affirms the success of the SR time-dependent method in a complex geological setting as Niger-Delta. The derivation of the volumetric table is to further enhance a more accurate exploration using the reflective seismic technique.

Acknowledgement

The authors appreciates the partial sponsorship of the research by Covenant University

Reference

[1] Piazza JL, Donati M, Martin FD, Castro J, Gordillo C and Belhouchet T. Multi-component 3D seismic–a successful fracture characterization in Algeria–interpretation of faults and fractures. In: 76th EAGE conference & exhibition, Amsterdam, 2014.

[2] Hatchell P and Bourne S. Rocks under strain: Strain induced time-lapse time-shifts are observed for depleting reservoirs. The Leading Edge, 2005; 24(12): 1222-1225.

[3] Farfour M and Yoon WJ. A review on multicomponent seismology: A potential seismic application for reservoir characterization, Journal of Advanced Research, 2016; 7(3):515-524.

[4] Li F, Zhou H, Jiang N, Bi J and Marfurt KJ. Q estimation from reflection seismic data for hydrocarbon detection using a modified frequency shift method, J. Geophys. Eng. 2015; 12: 577–586.

[5] Okal E and Mechler P. Bulletin of seismological society of America, 1973; 63(4): 1315-1319

[6] Anderson NL and Franseen EK. Differential compaction of Winnepegosis reefs: A seismic perspective, Geophysics, 2003; 56: 142–147.

[7] Ekweozor CM and Daukoru EM. Petroleum source-bed evaluation of Tertiary Niger-Delta; Discussion and Reply, AAPG Bulletin, 1984; 68: 387-394.

[8] Ritsema J, Rivera L, Komatitsch D, Tromp J, van Heijst, H. The effects of crust and mantle heterogeneity on PP/P and SS/S amplitude ratios, Geophys. Res. Lett., 2002; 29(10):72-1-72-4. doi:10.1029/2001GL013831.

[9] Ihianle OE, Alile OM, Azi SO, Airen JO and Osuji OU. Three dimensional seismic/well logs and structural interpretation over X-Y field in the Niger-Delta area of Nigeria. Science Technology, 2013; 3 (2): 47-54.

[10] Hospers J. Gravity field and structure of the Niger-Delta, Nigeria. West Africa. Geological society of American Bulletin, 1965; 76: 407-422.

[11] Short KC and Stauble AJ. Online of the geology of the Niger-Delta. American Society of Petroleum Geology Bulletin, 1967; 51: 761-779.
[12] Doust H and Omatsola E. Niger Delta, In, Edwards JD and Santogrossi PA. Eds., Divergent/Passive Margin Basins: AAPG Memoir 48: Tulsa, American Association of Petroleum Geologists, 1990; 48: 239-248.
[13] Evam BD, Harembourne J, Kamerling P, Knaap WA, Molley FA and Rowlands PH. Hydrocarbon habitat of the tertiary Niger Delta. AAPG Bull., 1978; 62:1–39.
[14] Nwankwo CN, Ohakwere-Eze M and Ebeniro JO. Hydrocarbon reservoir volume estimation using 3-D seismic and well log data over an X-field. Niger Delta Nigeria, Journal of Petroleum Exploration and Production Technology, 2015; 5 (4): 453-462.
[15] Kulke H. Regional Petroleum Geology of the World. Part II: Africa, America, Australia and Antarctica: Berlin, Gebrüder Borntraeger, 1995:143-172.
[16] Tuttle MLW, Charpentier RR, Brownfield ME. The Niger delta petroleum system: Niger delta province, Nigeria, Cameroon, and Equatorial Guinea, Africa. Open-file report 99-50-H. 1999.
[17] Barton N. Rock Quality, Seismic Velocity, Attenuation and Anisotropy, Taylor & Francis, London. 2007.
[18] Campbell KW. Estimates of Shear-Wave Q and κ_0 for Unconsolidated and Semi-consolidated Sediments in Eastern North America, Bulletin of the Seismological Society of America, 2009; 99 (4): 2365–2392.
[19] Hanks TC. Fmax. Bulletin of the Seismological Society of America, 1982; 72: 1867–1879.
[20] Papageorgiou AS and Ak K. A specific barrier model for the quantitative description of inhomogeneous faulting and the prediction of strong ground motion, Part II: Applications of the model, Bulletin of the Seismological Society of America, 1983; 73: 953–978.
[21] Ameloko AA and Owoseni AM. Hydrocarbon reservoir evaluation of X-field, Niger Delta using seismic and petrophysical data. International Journal of Innovation and Scientific Research, 2015; 15: 193-201.
[22] Aigbedion I, Aigbedion HO. Hydrocarbon Volumetric Analysis Using Seismic and Borehole Data over Umoru Field, Niger Delta-Nigeria. International Journal of Geosciences, 2011; 2: 179-183.

To whom correspondence should be addressed: emetere@yahoo.com